Intrinsic functional connectivity of motor and heteromodal association cortex predicts individual differences in regulatory focus

Nayoung Kim [ID][a,b], M. Justin Kim [ID][a,b,*], Timothy J. Strauman[c] and Ahmad R. Hariri [ID][c]

[a]Department of Psychology, Sungkyunkwan University, Seoul 03063, South Korea
[b]Center for Neuroscience Imaging Research, Institute for Basic Science, Suwon 16419, South Korea
[c]Department of Psychology and Neuroscience, Duke University, Durham, NC 27708, USA
*To whom correspondence should be addressed: Email: minuekim@skku.edu
Edited By: Jay Van Bavel

Abstract

Regulatory focus theory (RFT) describes two cognitive–motivational systems for goal pursuit—the promotion and prevention systems—important for self-regulation and previously implicated in vulnerability to psychopathology. According to RFT, the promotion system is engaged in attaining ideal goals (e.g. hopes and dreams), whereas the prevention system is associated with accomplishing ought goals (e.g. duties and obligations). Prior task-based functional magnetic resonance imaging (fMRI) studies have mostly explored the mapping of these two systems onto the activity of a priori brain regions supporting motivation and executive control in both healthy and depressed adults. However, complex behavioral processes such as those guided by individual differences in regulatory focus are likely supported by widely distributed patterns of intrinsic functional connectivity. We used data-driven connectome-based predictive modeling to identify patterns of distributed whole-brain intrinsic network connectivity associated with individual differences in promotion and prevention system orientation in 1,307 young university volunteers. Our analyses produced a network model predictive of prevention but not promotion orientation, specifically the subjective experience of successful goal pursuit using prevention strategies. The predictive model of prevention success was highlighted by decreased intrinsic functional connectivity of both heteromodal association cortices in the parietal and limbic networks and the primary motor cortex. We discuss these findings in the context of strategic inaction, which drives individuals with a strong dispositional prevention orientation to inhibit their behavioral tendencies in order to shield the self from potential losses, thus maintaining the safety of the status quo but also leading to trade-offs in goal pursuit success.

Keywords: regulatory focus, fMRI, goal pursuit, functional connectome

Significance Statement

Regulatory focus theory (RFT) proposes that people have two distinct motivational orientations—the promotion and prevention systems—when they pursue goals and regulate behaviors. Here, we implement modern neuroimaging approaches with a large functional magnetic resonance imaging (fMRI) dataset to investigate the brain correlates of classic cognitive–motivational systems for goal pursuit. Connectome-based predictive modeling identified a network model predictive of the prevention system highlighted by decreased intrinsic functional connectivity of the primary motor cortex. These results provide neurocognitive evidence supporting the RFT in the context of strategic inaction, which drives individuals with a strong dispositional prevention orientation to inhibit their behavioral tendencies in order to shield themselves from potential losses.

Introduction

It is well known that individual differences in motivational dispositions help shape people's approaches to pursuing goals, regulating behavior, and ensuring well-being (1). According to regulatory focus theory (RFT), two distinct motivational orientations are highly influential in helping to regulate personal goal pursuit (2, 3). Each can be characterized as a cognitive–motivational system organized around a desired end-state. The promotion system motivates individuals to pursue their "ideal self" by accomplishing hopes and dreams, based on a need for nurturance. The prevention system motivates individuals to pursue their "ought self" by fulfilling duties and obligations, based on a need for self-preservation. In descriptive terms, the promotion system motivates personal goal pursuit by "making good things happen" and

the prevention system motivates personal goal pursuit by "keeping bad things from happening" (4). Individual differences in regulatory focus have been shown to predict vulnerability to psychopathology, at both behavioral (5) and brain (6) levels of analysis.

RFT postulates that the motivational and affective consequences of failing or succeeding in goal pursuit are different for the two systems. Successful goal pursuit through a promotion orientation is associated with joy, happiness, and satisfaction, while failure is associated with sadness, disappointment, and frustration. In contrast, successful goal pursuit through a prevention orientation is associated with quiescence and calmness, while failure is associated with anxiety, worry, and agitation (7). Ongoing dysfunction in self-regulation increases risk for psychopathology, and a number of etiological pathways by which self-regulatory dysfunction generally and dysfunction of the promotion and/or prevention systems specifically might lead to disorders such as depression, generalized anxiety disorder, and eating disorders have been described (8, 9).

Identifying shared and unique functional brain correlates of these two systems offers an opportunity to not only further validate and refine RFT but also to leverage individual differences in goal pursuit to inform diagnosis and treatment. To date, the majority of studies examining the neural correlates of regulatory focus have employed task-based functional magnetic resonance imaging (fMRI) to identify patterns of activation associated with a promotion or prevention orientation primarily in terms of a priori regions of interest (along with examining the whole brain for exploratory purposes) (4, 6, 7, 10). Collectively, these studies have reported that individual differences in regulatory focus map onto activation patterns including subregions of the prefrontal cortex (PFC) supporting executive control and behavioral regulation as well as cortical midline structures supporting self-referential processes (11, 12). Detloff et al. (7) identified two partially overlapping sets of brain regions representing brain signatures of individualized promotion vs. prevention personal goal priming, using both traditional general linear model and tensorial probabilistic independent component analysis. The same partially overlapping sets of brain regions associated with promotion vs. prevention goal priming were found in a sample of healthy adolescents (13).

While such studies have linked the two RFT orientations with specific brain regions implicated in both normal and abnormal cognitive processes, a large body of emerging research has begun to reveal that individual differences in complex behavioral constructs such as promotion and prevention likely map onto widely distributed patterns of intrinsic brain network connectivity as well (14–16). Consistent with this perspective, Davis et al. (17) found a statistically reliable pattern of task-related functional connectomes associated with promotion and prevention in a sample of depressed individuals undergoing treatment. While that study was not designed a priori to examine network-level changes in functional connectivity before vs. after treatment, those authors found that treatments for depression specifically targeting the promotion system led to reliable changes in connectivity consistent with the RFT model. The work of Davis et al. (17) highlights the potential value of exploring how individual differences in the brain correlates of the promotion and prevention systems may be relevant for understanding the etiology and treatment of depression and related disorders. However, in order to identify functional connectivity correlates of emotional vulnerability based on RFT, normative analyses of how individual differences in promotion and prevention orientation predict functional connectivity are required. Furthermore, such normative analyses would be particularly useful if conducted using statistically robust, conceptually efficient, whole-brain analysis methods that provided strong tests of predictions regarding how individual differences in self-regulation predict features of fMRI data network models.

The present study aimed to expand on prior regional findings by investigating connectome-wide functional correlates of individual differences in regulatory focus. To address limitations resulting from small sample sizes and low statistical power (18, 19), we leveraged data from a large sample of 1,307 young adult university volunteers and derived reliable estimates of the whole-brain connectome using general functional connectivity (GFC), as we have done recently (20) to identify distributed brain connectivity correlates of individual differences in the dispositional use of emotion regulation strategies (21) and trait anger (22). Of note, GFC was derived from combining resting-state fMRI and task fMRI data in which its task events were regressed out, allowing more reliable estimates of intrinsic functional connectivity than when using resting-state fMRI alone by harnessing additional data points extracted from task fMRI data (20). We then used data-driven connectome-based predictive modeling (CPM) to predict individual differences in regulatory focus in held-out data from patterns of whole-brain intrinsic connectivity using k-fold cross-validation. Using a large fMRI dataset combined with connectome-based approaches, we first tested whether models built using multivariate patterns of whole-brain functional connectivity could predict individual differences in regulatory focus tendencies. Then, based on prior neuroimaging studies, we examined whether such predictive network models of regulatory focus included the PFC and cortical midline structures previously found to be associated with promotion and prevention. We hypothesized that, if promotion and prevention systems indeed share underlying brain correlates with executive control and behavioral regulation, then PFC and cortical midline structures should emerge as important components of the predictive network models of regulatory focus. Finally, taking advantage of the large sample size and data-driven approach, we sought to identify previously undiscovered brain regions and networks that may capture individual differences in promotion and prevention focus systems. By employing a data-driven exploratory framework, we aimed to provide important evidence for a holistic brain account of regulatory focus, which would complement and reconcile existing findings from smaller individual studies.

Results

Regulatory Focus Questionnaire

The Adolescent Regulatory Focus Questionnaire (RFQ) (23), an instrument designed for both high school and college-age individuals, was used as the continuous measure of chronic regulatory focus. For the RFQ success subscales, scores of promotion success ranged from 2.17 to 4.67 ($M = 3.58$, $SD = 0.39$) and prevention success from 1.83 to 4.5 ($M = 3.32$, $SD = 0.45$). For the history subscales, scores of promotion history ranged from 1.00 to 5.00 ($M = 4.03$, $SD = 0.92$) and prevention history from 0.00 to 5.00 ($M = 4.07$, $SD = 0.73$). The four RFQ subscales were not significantly correlated with age (promotion success, $r = 0.04$, $P = 0.145$; prevention success, $r = 0.043$, $P = 0.115$; promotion history, $r = 0.034$, $P = 0.223$; prevention history, $r = -0.013$, $P = 0.645$). Independent samples t tests showed significant sex differences in the RFQ

Table 1. Differences in scores of the RFQ subscales across sex and history of diagnosis for DX.

	Mean (SD)			Mean (SD)		
	Male	Female	t (P-value)	DX	Non-DX	t (P-value)
Promotion success	3.54 (0.39)	3.60 (0.38)	$t = -3.12$ ($P = 0.002$)	3.51 (0.41)	3.59 (0.38)	$t = 3.14$ ($P = 0.002$)
Prevention success	3.23 (0.43)	3.39 (0.45)	$t = -6.46$ ($P < 0.001$)	3.18 (0.46)	3.36 (0.44)	$t = 5.78$ ($P < 0.001$)
Promotion history	4.01 (0.86)	4.04 (0.97)	$t = -0.52$ ($P = 0.60$)	3.90 (1.00)	4.06 (0.90)	$t = 2.33$ ($P = 0.02$)
Prevention history	4.07 (0.68)	4.08 (0.77)	$t = -0.16$ ($P = 0.88$)	4.09 (0.69)	4.07 (0.74)	$t = -0.28$ ($P = 0.78$)

success subscales (promotion success, $t = -3.12$, $P = 0.002$; prevention success, $t = -6.46$, $P < 0.001$), such that both success scores were higher for women than men (Table 1). In addition, there were significant differences between individuals with a history of diagnosis for psychiatric disorders (DX) and non-DX groups (promotion success, $t = 3.14$, $P = 0.002$; prevention success, $t = 5.78$, $P < 0.001$; promotion history, $t = 2.335$, $P = 0.02$), with all three scores being lower for individuals with past or current diagnoses compared to those without (Table 1).

Connectome-based prediction of regulatory focus

We leveraged data from 1,307 young adults and generated whole-brain connectomes using GFC (20), which is derived from concatenating resting-state fMRI and task fMRI data, while regressing out task events from the latter. We then used data-driven CPM to predict individual differences in prevention success and promotion success scores using 10-fold cross-validation. To conduct CPM, every edge in the training set, including internetwork and intranetwork edges in GFC matrices, was correlated with RFQ scores to select predictive edges ($P < 0.01$). Then, edges that were positively and negatively correlated with RFQ scores were organized separately to construct positive and negative predictive network models, respectively. Correlation strengths of these selected edges in the positive/negative network models in the training set were summed and entered into a linear model trained to predict RFQ scores. Finally, the predictive performance of the trained model was assessed using the test set. To determine the significance of the models, null distribution was derived from 1,000 permutations wherein the participants and their RFQ scores were randomly shuffled to produce 1,000 random r-values. Nonparametric P-values were calculated by comparing the relative location of the actual r-value to the null distribution (see Materials and methods).

Connectome-based predictive model of prevention success

CPM analyses of the 1,307 functional connectomes (i.e. symmetric 264×264 functional brain connectivity matrices; see Materials and methods) revealed that the negative network model and the combined network model, but not the positive network model, significantly predicted prevention success scores (positive, $r = 0.04$, $P = 0.193$; negative, $r = 0.07$, $P = 0.008$; combined, $r = 0.12$, $P < 0.001$) after controlling for sex and DX. Permutation tests confirmed the prediction performance of the negative and the combined network models (negative, $P = 0.004$; combined, $P = 0.002$). Here, we focused on discussing the negative network model and the combined network model, as the positive network model was not statistically significant on its own.

Figure 1 and Table 2 summarize the significant edges in terms of functional networks, in which the edges generated from each model are distributed among 10 distinct functional networks (i.e. prefrontal, motor, insula, parietal, temporal, occipital, limbic, cerebellum, subcortical, brainstem) derived from the extent of their functional coactivation patterns (24). To elaborate, we found a total of 270 edges that negatively predicted prevention success scores in held-out (i.e. unseen) participants. Notably, 141 edges from the primary motor cortex accounted for more than half of the significant negative network edges. Edges from the parietal cortex (123 edges) and limbic cortex (77 edges) accounted for the second and third most edges contributing to the negative network. Nodes connecting these edges of the primary motor cortex and the parietal cortex were mostly located within the somatomotor network and the cingulo-opercular network, including paracentral lobule, anterior cingulate, precentral gyrus, supramarginal gyrus, and midcingulate. On the other hand, supporting the prediction that cortical midline structures would emerge as important components of the predictive network model for regulatory focus, nodes within the default mode network (DMN), such as middle temporal gyrus, parahippocampal gyrus, precuneus, midcingulate, and orbitofrontal cortex, contributed to edges of the limbic cortex (Table 2). Among these edges, 53 edges connecting the primary motor and parietal cortex ranked first in terms of connection frequency among all lobes, and 39 edges connecting nodes within the primary motor cortex ranked second. Overall results remain unchanged when extraversion and neuroticism personality traits ($n = 1,306$; measured using the NEO-PI-R scale) (25), which are known to be modestly associated with regulatory focus (26), were included in the model as additional covariates (positive, $r = 0.02$, $P = 0.539$; negative, $r = 0.08$, $P = 0.003$, permuted $P = 0.005$; combined, $r = 0.12$, $P < 0.001$, permuted $P < 0.001$).

Connectome-based predictive model of promotion success

No functional connectivity network showed significant prediction performance for promotion success scores after controlling for sex and DX, as well as extraversion and neuroticism.

Discussion

Seeking to extend existing knowledge regarding the brain signatures of promotion and prevention, we presented a predictive brain network model of individual differences in regulatory focus, generated from whole-brain functional connectomes of 1,307 young adults. Our data-driven CPM analyses revealed multivariate patterns of functional network connectivity significantly predictive of individual differences in prevention but not promotion success. Notably, stronger prevention success scores were predicted by reduced intrinsic functional connectivity of not only heteromodal association cortices in parietal and limbic networks but also primary motor cortex. These results were not explained by individual differences in personality traits such as extraversion or neuroticism, which is not surprising given the likelihood that regulatory focus and temperament-based traits are both developmentally and functionally distinct (27). Within the CPM-derived
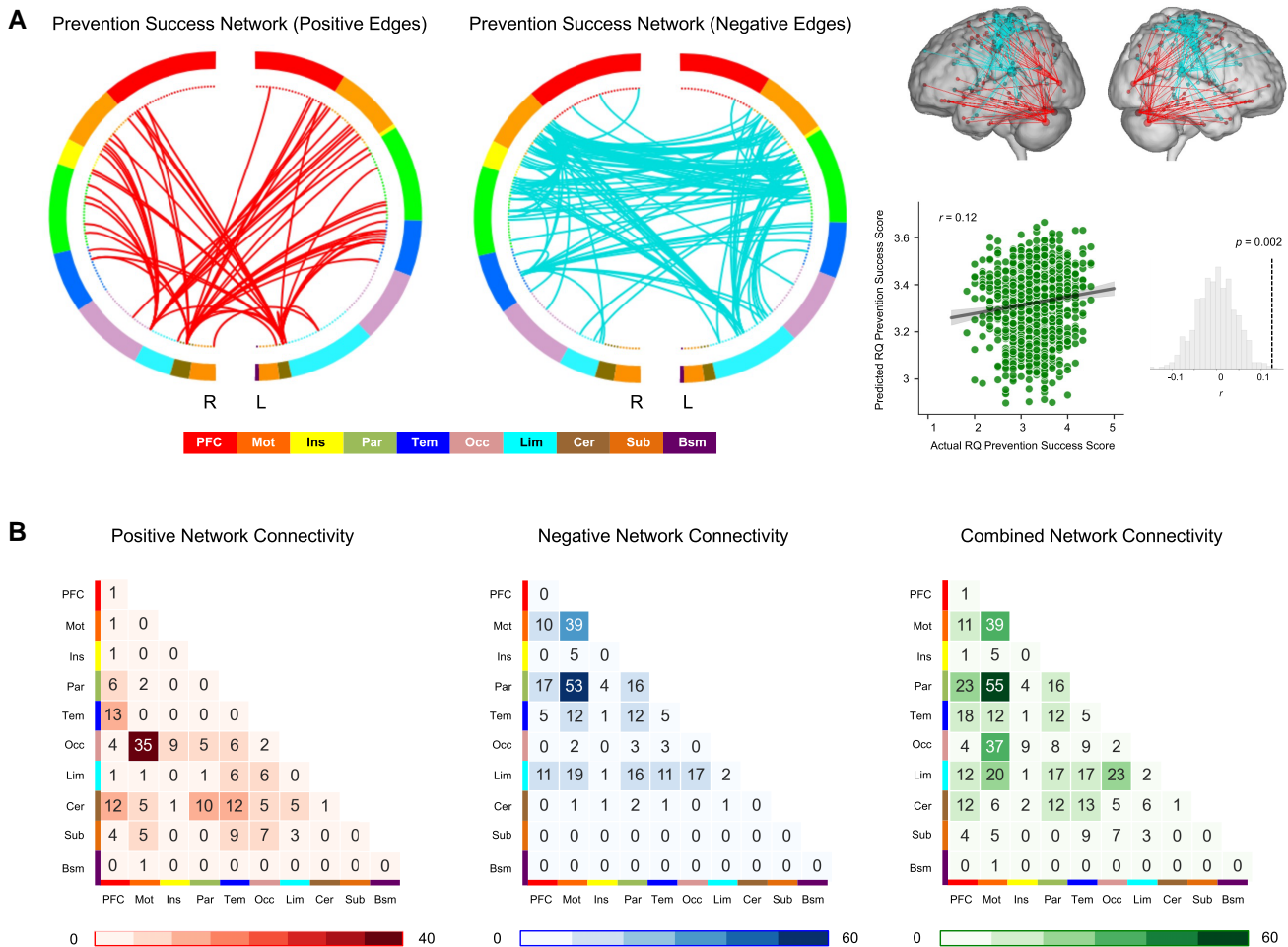
Fig. 1. Connectome-based prediction model of prevention success. A) Combined positive and negative networks contributed to the prediction of prevention success (P = 0.002; 1,000 permutations). B) Contributions of each of 10 functional networks to prevention success prediction, summarized by positive, negative, and combined networks. The numbers in each cell denote the number of edges for each pair of networks. PFC, prefrontal cortex; Mot, motor cortex; Ins, insula; Par, parietal cortex; Tem, temporal cortex; Occ, occipital cortex; Lim, limbic cortex; Cer, cerebellum; Sub, subcortical regions; R, right; L, left.

predictive network, the primary motor cortex had the highest number of predictive connections with other nodes, especially with the parietal network, followed by connections between nodes within the motor cortex highlighting its functional importance in predicting prevention success scores.

The prominent role of the primary motor cortex in predicting prevention success scores is a novel finding and suggests that the prevention system's motivational properties as a "top-down" cognitive structure may be similar to those attributed to the behavioral inhibition system (BIS) (28), a "bottom-up" cognitive structure which primarily dictates inaction rather than action. Gray (28, 29) conceptualized two motivational pathways for regulating behavioral reactions that are elicited by environmental stimuli, the behavioral activation system (BAS) and the BIS. The BAS activates approach behaviors toward rewarding stimuli, whereas the BIS prompts inhibition behaviors toward stimuli that serve as threats or punishment (30). We have previously discussed the similarities and distinctions between the prevention system and the BIS, both neuroanatomically and in terms of adaptive significance: RFT postulates two cognitive/motivational systems for higher order strategic goal pursuit, whereas BAS and BIS are attuned to spatiotemporally local stimuli with evolutionary significance (27). Nonetheless, the motivational characteristics of

the BIS draw a parallel with the strategic avoidance of negative outcomes for a person motivated by prevention goal pursuit according to RFT. Both systems operate under an inhibitory motivation aimed at minimizing loss against potential threats (4, 31), and BIS scores are significantly correlated with prevention focus scores (32). In addition, a critical characteristic shared across the BIS and the prevention system is the use of *inaction* through which an individual strives to shield the self from potential losses, maintaining the safety of the status quo (33) even though that choice often comes at the cost of not pursuing opportunities for gains.

The finding that primary motor cortex activation was influential in predicting individual differences in the prevention system may be explained in a number of ways. Intriguingly, a recent study revealed the presence of multiple mind–body interfaces embedded within the human primary motor cortex (34). Using a deep phenotyping approach, Gordon et al. identified intereffector areas between traditional effector-specific areas within the primary motor cortex (i.e. motor homunculus). Unlike the canonical effector-specific areas, these intereffector areas exhibited dense connectivity with regions of the prefrontal, insular, and parietal cortex supporting executive control and behavioral regulation (35). As such, the authors labeled those

Table 2. Top 25 nodes in the negative predictive network with the most connections that contributed to predicting prevention orientation.

Node	MNI coordinates (xyz)			Network	Number of connections
R paracentral lobule	2	−28	60	Somatomotor	40
L rolandic operculum	−38	−33	17	Auditory	25
L paracentral lobule	−7	−33	72	Somatomotor	23
L ventral anterior cingulate	−14	−18	40	Somatomotor	20
R precentral gyrus	42	−20	55	Somatomotor	18
L paracentral lobule	−13	−17	75	Somatomotor	17
R superior temporal gyrus	65	−33	20	Auditory	16
L middle temporal gyrus	−46	−61	21	Default mode	12
L parahippocampal gyrus	−26	−40	−8	Default mode	12
L paracentral lobule	−7	−21	65	Somatomotor	11
R supramarginal gyrus	54	−28	34	Cingulo-opercular	11
L midcingulate cortex	−10	−2	42	Cingulo-opercular	10
R superior frontal gyrus	19	−8	64	Cingulo-opercular	10
R postcentral gyrus	29	−39	59	Somatomotor	10
R supplementary motor area	13	−3	75	Somatomotor	9
L precentral gyrus	−38	−27	69	Somatomotor	8
R supplementary motor area	10	−2	45	Somatomotor	8
R postcentral gyrus	47	−30	49	Somatomotor	8
L precuneus	−11	−56	16	Default-mode	8
L midcingulate cortex	−2	−37	44	Default-mode	8
L rolandic operculum	−55	−9	12	Auditory	8
L precuneus	−7	−52	61	Somatomotor	7
R insula	36	−9	14	Somatomotor	7
R precentral gyrus	29	−17	71	Somatomotor	6
L anterior orbitofrontal cortex	−21	41	−20	Unknown	6

intereffector areas as mind–body interfaces supporting the dynamic top-down modulation of goal-directed actions through direct motor control (34). That logic potentially fits the nature and neurocognitive structure of the two motivational systems postulated by RFT.

It is thus possible that our CPM-derived predictive model reflects a propensity for *modulation of action*, with a bias toward inaction as a default, among individuals with greater prevention orientation. Such an explanation is consistent with the behavioral literature on RFT, wherein promotion-oriented goal pursuit is characterized by approach behavior that becomes more intense as the individual nears the goal, whereas prevention-oriented goal pursuit relies on behavioral strategies that minimize risk and potential exposure to losses. In other words, the weaker intrinsic functional connectivity between the primary motor cortex and heteromodal association cortices, especially the parietal cortex, that characterizes prevention-oriented individuals might reflect their behavioral and motivational tendencies for "strategic inaction" that is intended to maintain one's present state in order to prevent catastrophic loss. Conversely, individuals with stronger connectivity between these areas may have a lower threshold for goal-directed action (22). Recent discoveries of greater suppression of the motor cortex in individuals with higher BIS scores and less sensorimotor inhibition for individuals with lower BIS scores when facing threats also support this possibility (36, 37). Moreover, these empirical reports are consistent with the theoretical account linking the BIS system with motor inhibition (38). Interestingly, Amodio et al. (39) also applied that theoretical framework to interpreting distinctions between specific features of an electroencephalogram (EEG)/event-related potential (ERP) dataset that predicted promotion vs. prevention focus. Overall, our study provides data-driven evidence that further supports the connection between dispositional regulatory focus and inhibition of behavioral tendencies, particularly as associated with discriminant patterns of distributed whole-brain intrinsic network connectivity.

Supporting our hypothesis, the PFC and cortical midline structures emerged as important nodes within the predictive network model of regulatory focus. Together with the motor and parietal networks, the connectivity of nodes located within the DMN, such as the middle temporal gyrus, parahippocampal gyrus, precuneus, midcingulate, and orbitofrontal cortex, also contributed to the prediction of prevention success. These results fit well with the recently highlighted functional role of the DMN in the context of task performance (40). Moreover, in a recent study by Gale et al. (41), the interplay between the DMN and motor cortex was shown to promote goal-directed adaptation by controlling motor behavior via a top-down process. This study places our findings in proper context, as reduced functional connectivity between association cortices—especially the default mode and fronto-parietal networks—and the motor cortex during a sensorimotor adaptation task was related to poorer performance in action learning (41). Given that BIS has been shown to impair action learning task performance with regard to goal-oriented behavior (42, 43), our connectome-based predictive model of prevention success may indeed reflect the tendency for behavioral inhibition that is in line with the role of the motor-association connections to control action with higher order modulation (41).

The connectivity of nodes located within the DMN also extends previous task-based fMRI studies reporting associations between regulatory focus and activation of cortical midline structures supporting self-referential processes (44). In general, these prior studies suggest that rather than each regulatory focus domain (i.e. promotion vs. prevention) being exclusively associated with specific brain regions, global activation of cortical midline structures is observed because the individual conceptualizes their identity and a sense of self when they are processing their regulatory goal and its representations (4). This assertion is supported by the findings of Detloff et al. (7) in healthy adults as well as Daffre et al. (13) in healthy adolescents.

Using this unbiased whole-brain approach, we found that the DMN, which is central in generating models of the self (12), was

associated with individual differences in prevention but not promotion orientation. Our results showed that weaker connectivity of the DMN with other regions predicted higher chronic prevention focus. This aligns with the cognitive motivational processes of individuals with high prevention focus, who tend to be motivated by responsibilities and obligations (e.g. "feeling good about following rules") (23) rather than ideals or accomplishments. Social neuroscience has established that the DMN is reliably associated with tendencies for self-reflection and judgment, which are self-regulatory strategies more amenable to prevention ("don't make a mistake") than promotion ("take a chance"). At a strategic-interpersonal level, prevention orientation also leads to a sense of alleviation when adhering to directions or external circumstances, even when they are not in line with or go against the will of the individual, motivating behaviors such as readily following a given set of rules (45, 46). In this light, our findings could be understood as signifying that the association of prevention orientation with weaker functional connectivity of the DMN and other cortical midline structures also has the effect of limiting the extent to which the sense of self exerts an influence on other brain networks including the motor cortex.

We note that our analysis did not reveal a corresponding pattern of functional connectivity associated with the promotion system, which could be due to the nature of the promotion-goal pursuit that may not require cognitive processes complex enough to be captured at the brain network level. Individuals with high promotion orientation tend to act in order to pursue their desired ideal state in the presence of an interpersonal or environmental cue for attainment, which does not require self-reflection or consideration of morals and societal values (45). We speculate that the relatively straightforward and transitory motivational process of the promotion system is not as readily detected from the goal-free brain states (i.e. with no specific potential positive outcome made salient to each participant) that we examined in the present study.

Because our study employed a data-driven predictive modeling approach that reliably estimated whole-brain intrinsic functional network connectivity in a large sample (>1,000), we were able to address some important limitations of prior studies. First, small sample sizes (<100) often found in imaging studies are nonoptimal for achieving the statistical power necessary to detect small effects in individual differences research using fMRI (18, 19). Second, as described above, the majority of prior studies of regulatory focus have relied on a priori hypotheses concerning the prefrontal and cortical midline structures as brain regions of interest. Third, many task-based fMRI measures have poor test–retest reliability, which limits the ability to identify individual differences in brain–behavior associations (47). Nevertheless, one limitation of our study is the potential generalizability of our findings. The Duke Neurogenetics Study (DNS) data were collected from high-functioning young adult university students in the United States, so that it would be premature to assume that the same findings would be replicated in samples drawn from the general population. We recognize the need for future studies to validate and further investigate the present phenomenon in population-representative datasets. We note that this endeavor has become especially important in light of a recent report suggesting that brain-wide association studies require very large samples ((19); but see also Refs. (48, 49)).

To summarize, our data-driven, exploratory CPM of data from a large sample identified reliable patterns of intrinsic network functional connectivity predictive of individual differences in prevention but not promotion orientation toward goal pursuit.

Consistent with prior region of interest task-based fMRI findings, our analyses demonstrated that variability in the intrinsic functional connectivity of networks supporting executive control and behavioral regulation predicted prevention-oriented goal pursuit. More importantly, our data-driven whole-brain approach identified a previously unreported contribution of variability in the intrinsic connectivity of primary motor cortex in predicting individual differences in prevention-oriented goal pursuit. This finding helps deepen our understanding of individual differences in prevention-oriented goal pursuit orientation as reflecting patterns of intrinsic functional connectivity of motor control consistent with strategic inaction as a behavioral default. Moreover, this novel finding highlights the potential for data-driven whole-brain connectome analyses to reveal previously unknown links between brain and behavior that ultimately may extend our understanding of vulnerability to psychopathology.

Materials and methods
Participants

Data from 1,307 university student volunteers (751 women, 19.7 ± 1.3 years of age) who successfully completed the DNS between January 2010 and November 2016 were included in the present analyses. All participants provided written informed consent. The study protocol was approved by the Duke University Medical Center Institutional Review Board. To be eligible for the DNS, participants were required to be free of the following conditions: (i) medical diagnoses of cancer, stroke, head injury with loss of consciousness, untreated migraine headaches, diabetes requiring insulin treatment, chronic kidney, or liver disease; (ii) use of psychotropic, glucocorticoid, or hypolipidemic medication; and (iii) conditions affecting cerebral blood flow and metabolism (e.g. hypertension). Exclusion criteria did not include history of diagnosis for psychiatric disorders classified by the *Diagnostic and Statistical Manual of Mental Disorders, Fourth Edition* (50). Past or current diagnosis information is summarized in the Supplementary Information (Table S1). Participants self-reported as being White or Caucasian ($n = 652$), Black or African American ($n = 155$), Asian ($n = 356$), American Indian or Alaska Native ($n = 3$), Multiracial ($n = 102$), and other ($n = 39$), as well as Hispanic/Latino ($n = 134$). As the DNS followed a standardized procedure, we note that the following description of the methods is also described elsewhere (22, 51).

Regulatory focus

The Adolescent RFQ (23) was used as the continuous measure of chronic regulatory focus. The questionnaire is a minimally adapted version of the RFQ (45), which measures individual differences in orientation to promotion and prevention goals. The Adolescent RFQ consisted of 22 Likert-style items from four subscales: promotion history, prevention history, promotion success, and prevention success. The two history subscales evaluate the extent of socialization as a child to construe situations in terms of each orientation goal, while the two success subscales evaluate the extent to which the individual feels a sense of pride and well-being from pursuing each orientation goal. Sample items include, "My parents celebrated my accomplishments" (promotion history), "My parents pointed out possible dangers" (prevention history), "I become more motivated by accomplishments" (promotion success), and "I am feeling good about following rules" (prevention success). Due to the previously documented psychometric instability of the history subscales, our analyses focused on the

success subscales following the strategy employed in previous studies (4, 31, 45).

fMRI data acquisition

Each participant was scanned using one of the two identical research-dedicated GE MR750 3T scanner equipped with high-power high-duty-cycle 50-mT/m gradients at 200 T/m/s slew rate, and an eight-channel head coil for parallel imaging at high bandwidth up to 1 MHz at the Duke-UNC Brain Imaging and Analysis Center. A semiautomated high-order shimming program was used to ensure global field homogeneity. A series of 34 interleaved axial functional slices aligned with the anterior commissure-posterior commissure plane were acquired for full-brain coverage using an inverse-spiral pulse sequence to reduce susceptibility artifacts [repetition time (TR)/echo time (TE)/flip angle = 2,000 ms/30 ms/60; field-of-view (FOV) = 240 mm; 3.75 × 3.75 × 4 mm voxels; interslice skip = 0]. Four initial radiofrequency excitations were performed (and discarded) to achieve steady-state equilibrium. To allow for spatial registration of each participant's data to a standard coordinate system, high-resolution 3D T1-weighted structural images were obtained in 162 axial slices using a 3D Ax FSPGR BRAVO sequence (TR/TE/flip angle = 8.148 ms/3.22 ms/12°; voxel size = 0.9375 × 0.9375 × 1 mm; FOV = 240 mm; interslice skip = 0; total scan time = 4 and 13 s). In addition, high-resolution structural images were acquired in 34 axial slices coplanar with the functional scans and used for spatial registration for participants without Ax FSPGR BRAVO images (TR/TE/flip angle = 7.7 s/3.0 ms/12; voxel size = 0.9 × 0.9 × 4 mm; FOV = 240 mm, interslice skip = 0). For each participant, two back-to-back 4-min 16-s (256 time points) rsfMRI scans were acquired. Participants were instructed to remain awake, with their eyes open during each resting-state scan. Participants also completed a battery of four task fMRI scans, which consisted of an emotional face-matching task (6:30 min, 195 time points), a card-guessing task (5:42 min, 171 time points), a working memory task (11:48 min, 354 time points), and a face-naming task (5:24 min, 162 time points). Detailed descriptions of these four tasks are provided in the supplementary material (SI Methods).

fMRI data preprocessing

Anatomical images for each subject were skull-stripped, intensity-normalized, and nonlinearly warped to a study-specific average template in the standard stereotactic space of the Montreal Neurological Institute (MNI) template using ANTs (52). Blood-oxygen-level-dependent (BOLD) time series for each subject were processed in AFNI (53). Images for each subject were despiked, slice time-corrected, realigned to the first volume in the time series to correct for head motion, coregistered to the anatomical image using FSL's Boundary-Based Registration (54), spatially normalized into MNI space using the nonlinear warp from the anatomical image, resampled to 2 mm isotropic voxels, and smoothed to minimize noise and residual difference in gyral anatomy with a Gaussian filter, set at 6-mm full-width at half-maximum. All transformations were concatenated so that a single interpolation was performed. Voxelwise signal intensities were scaled to yield a time series mean of 100 for each voxel. Motion regressors were created using each subject's six motion correction parameters (three rotation and three translation) and their first derivatives (55) yielding 12 motion regressors. White matter and cerebrospinal fluid nuisance regressors were created using CompCor (56). Images were bandpass filtered to retain frequencies between 0.008 and 0.1 Hz, and volumes exceeding 0.5 mm framewise displacement or 2.5 standardized temporal derivative of root mean square (RMS) variance over voxels (DVARS)

were censored (57). All 1,307 participants had more than or equal to 229 time points left after censoring. Nuisance regression, bandpass filtering, and censoring for each timeseries were performed in a single processing step using AFNI's 3dTproject.

Functional network construction

After preprocessing, a whole-brain functional connectivity matrix (i.e. functional connectome) was constructed for each subject. Network nodes were defined using the Power 264-node brain atlas (58), which were further assigned to 10 functional networks (59) including prefrontal, motor, insula, parietal, temporal, occipital, limbic, cerebellum, subcortical, and brainstem lobe using BioImage Suite. To extract time-series data from each node, the atlas was warped from MNI space into individual-subject space. In order to compute GFC, average time-series data were extracted independently from each node per scan session. In the case of task fMRI data, we use AFNI's *3dTproject* to regress out the effects of tasks from the four task-based scans by adding task events as additional nuisance variables. The time series from rsfMRI and task-regressed fMRI data were concatenated and recombined for each participant to build GFC (20). Pairwise correlation was calculated for all possible pairs of nodes, and the resulting Pearson correlation coefficients were Fisher's z-transformed to yield symmetric 264 × 264 connectivity matrices. Each cell of the matrix represents the functional connection of corresponding edges.

Connectome-based predictive modeling

Based on the whole-brain GFC, CPM (59) was conducted to predict individual differences in regulatory focus. Since the two success subscales of the Adolescent RFQ represent heterogeneous psychological properties for promotion and prevention orientation, we performed the general process of CPM (59) for each of the two subscale scores of the questionnaire, controlling for covariates including sex and history of diagnosis for psychiatric disorders (DX). First, the data were separated into a training dataset and a test dataset (see below for details). Then, every edge in GFC matrices and the subscale scores from participants in the training dataset were correlated to select predictive edges which were most significantly correlated with behavioral variables. Here, we computed Spearman's rank correlation coefficients, and identified positively correlated edges and negatively correlated edges separately to construct positive and negative predictive networks ($P < 0.01$). Correlation strengths of these selected edges in each network were then summed to create single-subject statistics for each participant, which were entered into a training model that explained the Adolescent RFQ linearly. Finally, the linear model established with the training set was applied to the participants in the test set (i.e. held-out data) to predict their RFQ scores.

The test dataset and the training dataset that are required for model building were generated using *k*-fold cross-validation framework. Specifically, we arranged 1,307 participants into 10 approximately equal-sized groups. One group of participants were left out for testing, and data from the remaining nine groups were used to construct the training model. Then, the predictive ability of this this training model was assessed by fitting it with the test dataset. This procedure was repeated with a different left-out group in each step such that all 10 groups of participants served the role of the test sample in an iterative manner. Predictive scores generated from this process were then compared against the observed scores of the participants to see how much

the two scores were correlated, which represents a measure of the predictive power of the model (16). Then, the significance of the model performance was evaluated based on its relative position along the null distribution derived from permutations. In detail, the participants and their RFQ scores were randomly shuffled 1,000 times, where the CPM procedure was performed each time to yield 1,000 random r-values. Finally, to calculate nonparametric P-values, the number of random r-values larger than the r-value of the original model was divided by 1,000.

Acknowledgments

Supplementary Material

Supplementary material is available at *PNAS Nexus* online.

Funding

Author Contributions

N.K., M.J.K., T.J.S., and A.R.H. designed the research, interpreted the results, and wrote the paper. N.K. and M.J.K. analyzed the data and prepared all figures. T.J.S and A.R.H. revised the paper. All authors reviewed the manuscript.

Data Availability

The data that support the findings of this study are available on request (see data sharing procedures through our website https://www.haririlab.com/projects/procedures.html). The data are not publicly available because they contain information that could compromise research participant privacy/consent.

References

1 Ryan RM, Deci EL. 2001. On happiness and human potentials: a review of research on hedonic and eudaimonic well-being. *Annu Rev Psychol*. 52:141–166.

2 Higgins ET. 1997. Beyond pleasure and pain. *Am Psychol*. 52:1281–1290.

3 Higgins ET. 1998. Promotion and prevention: regulatory focus as a motivational principle. *Adv Exp Soc Psychol*. 30:1–46.

4 Strauman TJ, *et al.* 2013. What shall I be, what must I be: neural correlates of personal goal activation. *Front Integr Neurosci*. 6:123.

5 Romer AL, Hariri AR, Strauman TJ. 2021. Regulatory focus and the p factor: evidence for self-regulatory dysfunction as a transdiagnostic feature of general psychopathology. *J Psychiatr Res*. 137:178–185.

6 Eddington KM, *et al.* 2009. Neural correlates of idiographic goal priming in depression: goal-specific dysfunctions in the orbitofrontal cortex. *Soc Cogn Affect Neurosci*. 4:238–246.

7 Detloff AM, Hariri AR, Strauman TJ. 2020. Neural signatures of promotion versus prevention goal priming: fMRI evidence for distinct cognitive–motivational systems. *Personal Neurosci*. 3:e1.

8 Karoly P. 2010. Psychopathology as dysfunctional self-regulation: when resilience resources are compromised. In: Reich JW, Zautra AJ, Hall JS, editors. *Handbook of adult resilience*. New York: The Guilford Press. p. 146–170.

9 Strauman TJ. 2017. Self-regulation and psychopathology: toward an integrative translational research paradigm. *Annu Rev Clin Psychol*. 13:497–523.

10 Eddington KM, Dolcos F, Cabeza R, Krishnan KR, Strauman TJ. 2007. Neural correlates of promotion and prevention goal activation: an fMRI study using an idiographic approach. *J Cogn Neurosci*. 19:1152–1162.

11 Northoff G, Bermpohl F. 2004. Cortical midline structures and the self. *Trends Cogn Sci*. 8:102–107.

12 Qin P, Northoff G. 2011. How is our self-related to midline regions and the default-mode network? *Neuroimage*. 57:1221–1233.

13 Daffre C, Detloff A, Brewster A, Strauman TJ. 2024. Neural signatures of promotion and prevention goal activation in adolescence. PsyArXiv. https://doi.org/10.31234/osf.io/d5u9t, preprint: not peer reviewed.

14 Cáceda R, James GA, Gutman DA, Kilts CD. 2015. Organization of intrinsic functional brain connectivity predicts decisions to reciprocate social behavior. *Behav Brain Res*. 292:478–483.

15 Dubois J, Galdi P, Paul LK, Adolphs R. 2018. A distributed brain network predicts general intelligence from resting-state human neuroimaging data. *Philos Trans R Soc Lond B Biol Sci*. 373:20170284.

16 Rosenberg MD, *et al.* 2016. A neuromarker of sustained attention from whole-brain functional connectivity. *Nat Neurosci*. 19:165–171.

17 Davis SW, *et al.* 2023. Network-level dynamics underlying a combined rTMS and psychotherapy treatment for major depressive disorder: an exploratory network analysis. *Int J Clin Health Psychol*. 19:100382.

18 Dubois J, Adolphs R. 2016. Building a science of individual differences from fMRI. *Trends Cogn Sci*. 20:425–443.

19 Marek S, *et al.* 2022. Reproducible brain-wide association studies require thousands of individuals. *Nature*. 603:654–660.

20 Elliott ML, *et al.* 2019. General functional connectivity: shared features of resting-state and task fMRI drive reliable and heritable individual differences in functional brain networks. *Neuroimage*. 189:516–532.

21 Burr DA, *et al.* 2020. Functional connectivity predicts the dispositional use of expressive suppression but not cognitive reappraisal. *Brain Behav*. 10:e01493.

22 Kim MJ, Elliott ML, Knodt AR, Hariri AR. 2022. A connectome-wide functional signature of trait anger. *Clin Psychol Sci*. 10:584–592.

23 Strauman TJ, *et al.* 2006. Self-system therapy as an intervention for self-regulatory dysfunction in depression: a randomized comparison with cognitive therapy. *J Consult Clin Psychol*. 74:367–376.

24 Shen X, Tokoglu F, Papademetris X, Constable RT. 2013. Groupwise whole-brain parcellation from resting-state fMRI data for network node identification. *Neuroimage*. 82:403–415.

25 Costa PT, McCrae RR. 1992. *Revised NEO Personality Inventory (NEO-PI-R) and NEO Five-Factor Inventory (NEO-FFI) professional manual*. Odessa (FL): Psychological Assessment Resources.

26 Lanaj K, Chang C-H, Johnson RE. 2012. Regulatory focus and work-related outcomes: a review and meta-analysis. *Psychol Bull*. 138:998–1034.

27 Strauman TJ, Wilson WA. 2010. Individual differences in approach and avoidance: behavioral activation/inhibition and regulatory focus as distinct systems. In: Hoyle R, editor. *Handbook of self-regulation and personality*. New York: The Guildford Press. p. 447–473.

28 Gray JA. 1976. The behavioural inhibition system: a possible substrate for anxiety. In: Feldman MP, Broadhurst AM, editors. *Theoretical and experimental bases of behaviour modification*. London: Wiley. p. 3–41.

29 Gray JA. 1994. Three fundamental emotion systems. In: Ekman P, Davidson RJ, editors. *The nature of emotion*. New York: Oxford University Press. p. 243–247.

30 Depue RA, Collins PF. 1999. Neurobiology of the structure of personality: dopamine, facilitation of incentive motivation, and extraversion. *Behav Brain Sci*. 22:491–569.

31 Scult M, *et al*. 2017. Individual differences in regulatory focus predict neural response to reward. *Soc Neurosci*. 12:419–429.

32 Ouschan L, Boldero JM, Kashima Y, Wakimoto R, Kashima ES. 2007. Regulatory focus strategies scale: a measure of individual differences in the endorsement of regulatory strategies. *Asian J Soc Psychol*. 10:243–257.

33 Crowe E, Higgins E. 1997. Regulatory focus and strategic inclinations: promotion and prevention in decision-making. *Organ Behav Hum Decis Process*. 69:117–132.

34 Gordon EM, *et al*. 2023. A somato-cognitive action network alternates with effector regions in motor cortex. *Nature*. 617:351–359.

35 Dosenbach NUF, *et al*. 2006. A core system for the implementation of task sets. *Neuron*. 50:799–812.

36 Borgomaneri S, Vitale F, Avenanti A. 2017. Behavioral inhibition system sensitivity enhances motor cortex suppression when watching fearful body expressions. *Brain Struct Funct*. 222: 3267–3282.

37 Botta A, *et al*. 2022. Sensorimotor inhibition during emotional processing. *Sci Rep*. 12:1–13.

38 Amodio DM, Master SL, Yee CM, Taylor SE. 2008. Neurocognitive components of the behavioral inhibition and activation systems: implications for theories of self-regulation. *Psychophysiology*. 45: 11–19.

39 Amodio DM, Shah JY, Sigelman J, Brazy PC, Harmon-Jones E. 2004. Implicit regulatory focus associated with asymmetrical frontal cortical activity. *J Exp Soc Psychol*. 40:225–232.

40 Smallwood J, *et al*. 2021. The default mode network in cognition: a topographical perspective. *Nat Rev Neurosci*. 22:503–513.

41 Gale DJ, *et al*. 2022. Distinct patterns of cortical manifold expansion and contraction underlie human sensorimotor adaptation. *Proc Natl Acad Sci U S A*. 119:e2209960119.

42 Eriksson LJ, Jansson B, Lisspers J, Sundin Ö. 2016. The interactive effect of the behavioral inhibition system (BIS) and response inhibition on accuracy in a modified stop-signal task. *Pers Individ Differ*. 97:198–202.

43 Sadler JR, Shearrer GE, Papantoni A, Gordon-Larsen P, Burger KS. 2020. Behavioral and physiological characteristics associated with learning performance on an appetitive probabilistic selection task. *Physiol Behav*. 223:112984.

44 Beer JS, Ochsner KN. 2006. Social cognition: a multi-level analysis. *Brain Res*. 1079:98–105.

45 Higgins ET, *et al*. 2001. Achievement orientations from subjective histories of success: promotion pride versus prevention pride. *Eur J Soc Psychol*. 31:3–23.

46 Semin GR, Higgins T, De Montes LG, Estourget Y, Valencia JF. 2005. Linguistic signatures of regulatory focus: how abstraction fits promotion more than prevention. *J Pers Soc Psychol*. 89:36–45.

47 Elliott ML, *et al*. 2020. What is the test–retest reliability of common task-functional MRI measures? New empirical evidence and a meta-analysis. *Psychol Sci*. 31:792–806.

48 Cecchetti L, Handjaras G. 2022. Reproducible brain-wide association studies do not necessarily require thousands of individuals. PsyArXiv. https://doi.org/10.31234/osf.io/c8xwe, preprint: not peer reviewed.

49 Spisak T, Bingel U, Wager T. 2022. Multivariate BWAS can be replicable with moderate sample sizes. *Nature*. 615:E4–E7.

50 American Psychiatric Association. 1994. *Diagnostic and statistical manual of mental disorders*. 4th ed. Washington (DC): Author.

51 Kim MJ, Avinun R, Knodt AR, Radtke SR, Hariri AR. 2017. Neurogenetic plasticity and sex influence the link between corticolimbic structural connectivity and trait anxiety. *Sci Rep*. 7:1–8.

52 Klein A, *et al*. 2009. Evaluation of 14 nonlinear deformation algorithms applied to human brain MRI registration. *Neuroimage*. 46: 786–802.

53 Cox RW. 1996. AFNI: software for analysis and visualization of functional magnetic resonance neuroimages. *Comput Biomed Res*. 29:162–173.

54 Greve DN, Fischl B. 2009. Accurate and robust brain image alignment using boundary-based registration. *Neuroimage*. 48:63–72.

55 Satterthwaite TD, *et al*. 2013. An improved framework for confound regression and filtering for control of motion artifact in the preprocessing of resting-state functional connectivity data. *Neuroimage*. 64:240–256.

56 Behzadi Y, Restom K, Liau J, Liu TT. 2007. A component based noise correction method (CompCor) for BOLD and perfusion based fMRI. *Neuroimage*. 37:90–101.

57 Power JD, *et al*. 2014. Methods to detect, characterize, and remove motion artifact in resting state fMRI. *Neuroimage*. 84:320–341.

58 Power JD, *et al*. 2011. Functional network organization of the human brain. *Neuron*. 72:665–678.

59 Shen X, *et al*. 2017. Using connectome-based predictive modeling to predict individual behavior from brain connectivity. *Nat Protoc*. 12:506–518.